

The Trigger System of the H.E.S.S. Telescope Array

S. Funk^{a,*}, G. Hermann^a, J. Hinton^a, D. Berge^a,
K. Bernlöhner^a, W. Hofmann^a, P. Nayman^b, F. Toussenel^b,
P. Vincent^b

^a*Max-Planck-Institut für Kernphysik, P.O. Box 103980, D-69029 Heidelberg, Germany*

^b*Laboratoire de Physique Nucléaire et de Hautes Energies, IN2P3/CNRS, Universités Paris VI & VII, 4 place Jussieu, F-75252 Paris Cedex 05, France*

Abstract

H.E.S.S. – The High Energy Stereoscopic System – is a new system of large atmospheric Cherenkov telescopes for GeV/TeV γ -ray astronomy. This paper describes the trigger system of H.E.S.S. with emphasis on the multi-telescope array level trigger. The system trigger requires the simultaneous detection of air-showers by several telescopes at the hardware level. This requirement allows a suppression of background events which in turn leads to a lower system energy threshold for the detection of γ -rays. The implementation of the H.E.S.S. trigger system is presented along with data taken to characterise its performance.

1 Introduction

Present instruments in the field of ground-based γ -ray astronomy are sensitive to photons with energies above ~ 100 GeV. The most sensitive of these instruments are Imaging Atmospheric Cherenkov Telescopes (IACTs) or arrays of such telescopes. IACTs image the Cherenkov light emitted by atmospheric particle showers initiated by cosmic γ -rays or hadrons. Fast photon detectors and electronics are required to distinguish the Cherenkov light from such air-showers from fluctuations of the night sky background light (NSB). Photomultiplier tubes (PMTs) are currently the most appropriate light sensors for IACT cameras. For γ -ray initiated showers the light yield at the ground

* Corresponding author, Stefan.Funk@mpi-hd.mpg.de

is roughly proportional to the energy of the primary particle. γ -ray showers are observed against a background of much more numerous hadronic showers. This background can be greatly reduced using the morphology of air-shower images. Image analysis provides estimates of the direction and energy of the primary particle.

The pioneering experiment in this field was the Whipple telescope [1], which achieved an energy threshold of around 350 GeV. Significant improvement in sensitivity and energy resolution of the IACT technique was achieved in the last generation of instruments by HEGRA [2] through the introduction of stereoscopy, where showers are imaged simultaneously by multiple Cherenkov telescopes. This technique provides a more accurate measurement of shower parameters such as energy and direction and leads to an improved γ -ray sensitivity. The current generation of instruments aims to lower the energy threshold to below 100 GeV. All new major installations are based on the stereoscopic approach (H.E.S.S. [3], VERITAS [4] and CANGAROO-III [5]) or plan to adopt stereoscopy (MAGIC, phase II [6]).

The High Energy Stereoscopic System (H.E.S.S.) is located in Namibia (Africa) at an altitude of 1800 metres. Phase I consists of four Cherenkov telescopes, each of 107 m² mirror area [7]. The telescopes are arranged on a square with 120 m sides. The cameras of the telescopes are each equipped with 960 pixels, covering a 5° field of view with a pixel size of 0.16° [8]. The telescopes of the system were commissioned between June 2002 and December 2003. The trigger system of H.E.S.S. is designed to make optimum use of the stereoscopic approach. Simultaneous observation of an air-shower in multiple telescopes is required at the hardware level. This coincidence requirement reduces the rate of background events (for example single muons) significantly, enabling a reduction of the energy threshold of the system by a factor ~ 2 compared to single telescope operation.

This paper first discusses the triggering of Cherenkov telescopes in general, followed by a description of the H.E.S.S. trigger system. Technical measurements using air-showers are presented along with a discussion of the impact of the stereo trigger on the physics performance of the H.E.S.S. experiment.

2 Trigger and Readout of Cherenkov Telescopes

2.1 *Triggering Cherenkov Telescopes*

The triggering of Cherenkov telescopes makes use of the extremely short duration (a few nanoseconds) of the Cherenkov light signal from air-showers. A

typical requirement for triggering the readout of a telescope is that a minimum number of pixels exhibit a signal larger than a given threshold (typically a few photoelectrons) within a short time window, to reduce random triggers from the night sky background. Following a trigger, signals are digitised and read out, resulting in a dead-time ranging from a few 10 μ s to a few 10 ms, depending on the design of the data acquisition system.

The trigger rate (and therefore the dead-time) of a single telescope system is dominated by background events. For instruments with energy thresholds in the TeV range, hadronic air-showers produce the majority of this background. At the lower energy thresholds reached by telescopes of larger mirror area, single muons passing close to the Cherenkov telescope become a sizable part of the background.

In a system of telescopes, the requirement that two telescopes (separated e.g. by ~ 100 m) both trigger within a short time window leads to a significant reduction in the rate of background events. Since hadronic showers have a more inhomogeneous light pool, the coincidence requirement disfavors such events in comparison to γ -ray events. Single muons are almost completely rejected by a telescope multiplicity requirement.

Given this reduction in background and the advantages of stereoscopic reconstruction (see for example [9]), it is necessary to select multiple-telescope events at least for off-line analysis. In a system with non-negligible read-out dead-time it is desirable to select coincident events at the hardware level. A system level coincidence trigger has the additional advantages of greatly reducing the network, disc space, and CPU time requirements of the system. For these reasons a system level trigger was incorporated in the design of the H.E.S.S. project.

During commissioning of phase I of the H.E.S.S. telescope system, with two telescopes operational, some data were taken with independent telescope triggers and software matching of events based on GPS time-stamps (*software stereo data*). The system level trigger has been used for all data taking since July 2003.

2.2 Trigger and Readout of the H.E.S.S. cameras

The trigger of the H.E.S.S. cameras [8] is derived from a multiplicity trigger within overlapping *sectors*, each containing 64 pixels. A camera trigger occurs if the signals in M pixels within a sector (*sector threshold*) exceed a threshold of N photoelectrons (*pixel threshold*). The time-window for the multiplicity trigger is dictated by the minimum integrated charge over a programmable threshold. For a typical PMT pulse shape the effective trigger window is 1.3 ns

(with a jitter of 0.14 ns). This rather narrow gate is possible due to the sorting of PMTs by high voltage within the camera. This sorting minimises the time dispersion introduced by different PMT transit times. The narrow gate guarantees maximum NSB suppression.

The trigger sectors overlap to ensure a homogeneous trigger efficiency across the field-of-view of the camera. The sector and pixel thresholds are programmable and are in the range of a few photoelectrons for a minimum multiplicity of typically 2 to 4 pixels. The PMT signals are sampled using 1 GHz Analogue Ring Samplers (ARS) [11] with a ring buffer depth of 128 cells. Following a camera trigger, the ring buffer is stopped and the content of the ring buffer, within a programmable time window (normally 16 ns) around the signal, is digitised, summed and written to an FPGA buffer. This process takes $\approx 273 \mu\text{s}$. During the first 10 μs , it is possible to interrupt the digitisation with an external reset signal. In this case, the readout of the analogue memories is stopped and the sampling restarted. After digitisation, the transfer of all buffered data into a global FiFo memory requires another 141 μs . The total dead-time, including interrupt handling and data acquisition preprocessing is 446 μs for an event that is read out, or 5.5 μs for an event that is discarded.

After read out, the camera is ready for the next event. Further data processing within the camera is done asynchronously, including the transmission of data via optical fibre to the PC processor farm located in the control building.

3 The System Trigger of H.E.S.S.

3.1 Overview

The trigger of H.E.S.S. is a two-level system. At the first level, telescopes independently form *local triggers* (see section 2.2), at the second level a multi-telescope coincidence decision is made by the central trigger system (CTS). In addition to the formation of the system level trigger, the CTS is responsible for dead-time measurement and event synchronisation.

The H.E.S.S. CTS consists of hardware in a central station located in the control building of the array and of interface modules located in each camera. The central station is designed to serve up to 8 telescopes arranged into arbitrary sub-arrays, to accommodate expansion of the H.E.S.S. telescope system beyond phase I. The communication between the central station and the interface modules is done via an optical fibre system built from standard components with one duplex pair per telescope.

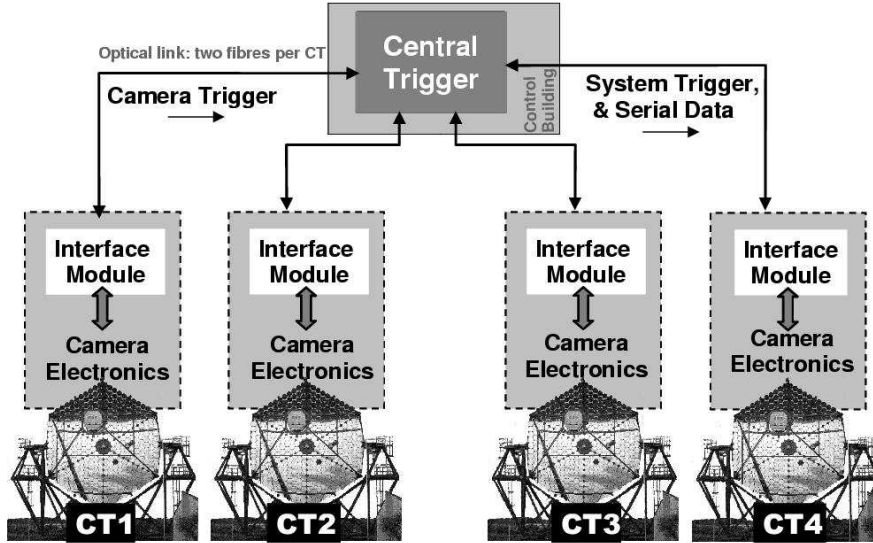


Fig. 1. Schematic of the data flow in of the H.E.S.S. central trigger system.

Information on all telescope triggers arrives at the central station. If a valid coincidence occurs, the central station distributes this information to all telescopes and the cameras of those telescopes which participated in this system event are read out. To enable the measurement of the system dead-time, cameras provide their current readout status together with the trigger signal (i.e. whether the camera is *busy* acquiring a previous event or *active* and able to read out this event). The camera trigger and readout status information is stored for each telescope on an event by event basis in a FiFo. From these data the dead-time of the system can be derived. The data flow between the cameras and the central trigger system is shown schematically in figure 1.

To provide a synchronisation mechanism, the CTS assigns for each event a unique, system-wide event number, which is distributed via the trigger hardware to all telescopes. The event number is read by the camera together with the pixel data of each telescope and is used in the process of building a system event from the individual telescope data. An absolute time-stamp for the system event is provided by a GPS clock in the central station.

3.2 Camera Interface

An interface module (illustrated schematically in figure 2) is contained within the body of each camera and is responsible for encoding and transmission of camera triggers and decoding and relaying pulses from the central station. TTL trigger pulses are received from the camera together with a TTL level

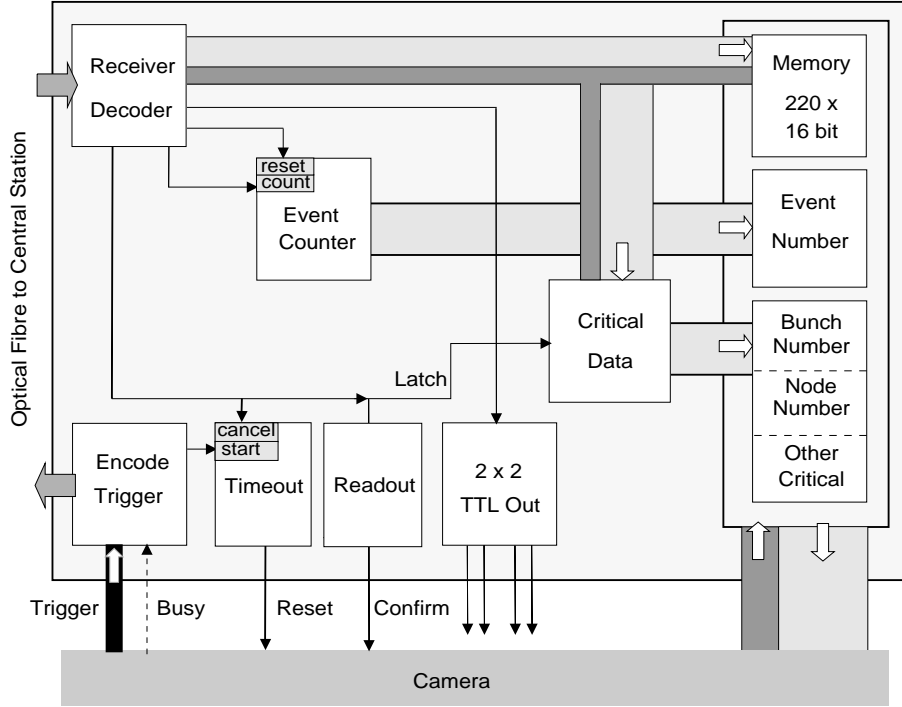


Fig. 2. Schematic illustration of the camera interface module of the H.E.S.S. system trigger. The trigger path is shown in black, data flow is shown in pale grey and addressing in darker grey. Pulses are shown as solid lines.

indicating the current readout status. This information is transformed into a width-encoded pulse which is sent via optical fibre to the central station.

Information from the central station is received via a second fibre. Two transmission types are used: a system trigger pulse and a serial data word used to control the interface module and pass data to the camera. The system trigger is also pulse width encoded: the telescopes that have sent active triggers receive *readout* pulses, and all other telescopes receive a *count* pulse. In either case a local event counter is incremented in the interface module and is, therefore, synchronised to the system event counter. In the case of a *readout* pulse, the event counter is latched into an output register on the interface module, where it is read by the camera electronics and written into the data stream.

If a telescope sends an active trigger but no system coincidence occurs, the interface module sends a reset signal to the camera after an adjustable delay, dictated by the round-trip time of pulses between the telescopes and the control building ($4.2 \mu\text{s}$) plus the time required to make a coincidence decision (330 ns). If a reset signal is sent, the camera discards the event and is immediately ready for a new trigger and readout.

The serial transmission mechanism is used to periodically reset the event counter and update synchronously a *bunch number* and a *node number* in the interface modules of all telescopes. Both numbers are latched into the

memory of the interface module by the arrival of a readout pulse. The node number identifies to which node of the computer farm data should be sent for processing. The combination of the event counter and bunch number provides a unique system wide event identifier which is used for event-building at the farm computer specified as the receiving node.

In case a count pulse is lost, the bunch number and the reset of the event counter ensure that the synchronisation of events is recovered after a few seconds.

3.3 Central Station

The central station hardware consists of the following custom-built VME modules:

- Optical/TTL converter module
- Programmable delay module
- Coincidence trigger module
- Telescope trigger scaler

together with a GPS clock for absolute timing.

Incoming pulses from the optical fibre are converted in the optical converter to TTL pulses. The programmable delay (up to 1 μ s in steps of 1 ns) compensates for the (fixed) delays due to different optical fibre lengths and the (varying) differences in the arrival times of the Cherenkov light front at the individual telescopes. Calculation of the variable component is based on the current pointing direction of the telescope system.

After this delay compensation, telescope triggers enter the coincidence module where they are duplicated and follow two paths (see figure 3). The coincidence path checks if the system trigger condition is fulfilled within the coincidence window, without regard to the busy status of the telescope. The coincidence window is generated by adjusting the width of the incoming pulses to a programmable duration and requiring a minimum overlap of 10 ns. The trigger condition is checked using a programmable lookup table in which all allowed coincidence patterns are stored. This system has the advantage that independent sub-arrays of telescopes can be served simultaneously. The second path identifies the active or busy status of the telescopes and writes this information (together with the event and bunch numbers and a GPS time-stamp) into a FiFo for every system coincidence. Once this information has been written to the FiFo, the trigger module is ready to accept new triggers, about 330 ns after the coincidence occurred. The FiFo has a depth of 16000 events and is read out asynchronously. The readout time per event is 4.5 μ s, allowing for a

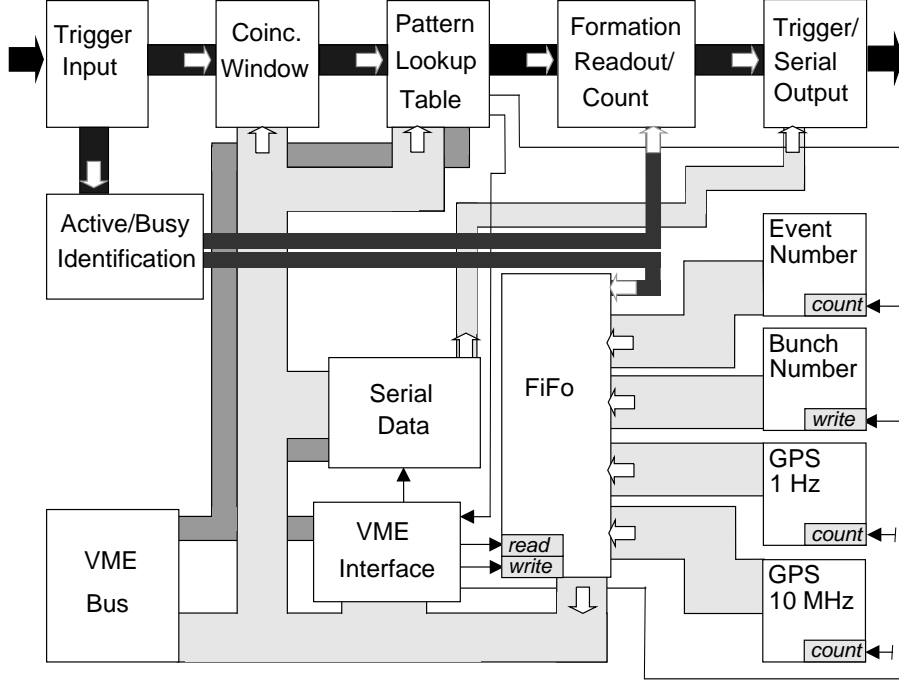


Fig. 3. The flow of information in the H.E.S.S. central coincidence module. The two trigger paths are shown in black. Data flow is shown in pale grey and addressing in darker grey. Pulses are shown as solid lines.

maximum sustained rate of 200 kHz. When a system trigger occurs, *readout* and *count* pulses are sent via the optical converter module to the interface modules in each camera.

Event time-stamps are provided by a commercial *GPS167 Meinberg* GPS receiver. This clock provides 1 Hz and 10 MHz TTL signals synchronised to the UTC second. These signals are used as inputs for the corresponding counters in the coincidence module to provided relative timing. An absolute reference time is obtained by serial readout of a complete date/time string from the clock via RS232. The precision of the system has been verified by simultaneous operation of two such clocks and using the optical pulsed emission of the Crab Pulsar as an absolute reference [12]. The long term accuracy of the system is $< 2\mu\text{s}$.

Only coincident events are recorded by the coincidence module. Individual telescope trigger rates (both *active* and *busy*) are monitored separately using a custom-built VME scaler.

Extensive laboratory tests of the central trigger system showed error rates of less than 10^{-8} in all aspects of system operation, including serial data transmission over optical fibre and trigger pattern identification and readout.

4 System Trigger Characterisation

Since December 2003, the H.E.S.S. detector has been operating as a four telescope system using the system trigger described here¹. During March 2004, a number of technical measurements were made with the aim of characterising the complete H.E.S.S. trigger. These measurements used hadronic air-shower events to provide an end-to-end test of the system and are described in detail below.

4.1 Telescope Delays and Coincidence Window

An efficient and unbiased multi-telescope trigger must provide a coincidence window wide enough that no valid Cherenkov coincidences are lost. On the other hand, the window should be narrow enough to avoid an unacceptable rate of random telescope coincidences. The minimum achievable window is dictated by the intrinsic spread in the arrival times of telescope triggers at the central station. This spread results mainly from the width and curvature of the Cherenkov wave front and the field-of-view of the cameras, and for H.E.S.S. has an r.m.s. of close to 10 ns. The telescope trigger delay compensation – which depends on the pointing direction – is updated frequently enough (in steps of 1 ns) that there is no additional contribution to this spread.

To demonstrate the correct calculation of the compensation delays, the following procedure was applied to all pairs of telescopes. Air-shower data was taken with telescopes tracking an astronomical target. A rather narrow coincidence window was used and a varying offset was artificially added to the programmed delays. The resulting curve of system rate versus delay offset for one pair of telescopes is shown in figure 4 for two different coincidence windows.

For the 20 ns window, the delay offset which results in a maximum system rate is 1.5 ± 0.5 ns. The 40 ns window is significantly wider than the intrinsic spread in arrival times (≈ 10 ns rms) and hence a clear plateau is evident, where the system rate is insensitive to an offset in the telescope delays.

To avoid any bias from the system trigger on the selection of showers, the operating coincidence gate is set to 80 ns. For typical individual telescope rates of 1 kHz, this window introduces an acceptable accidental coincidence rate of 1 Hz for the 4-telescope system.

¹ The system level trigger was installed in July 2003 and operated until December 2003 with 2-3 telescopes, and since then with the complete 4-telescope system.

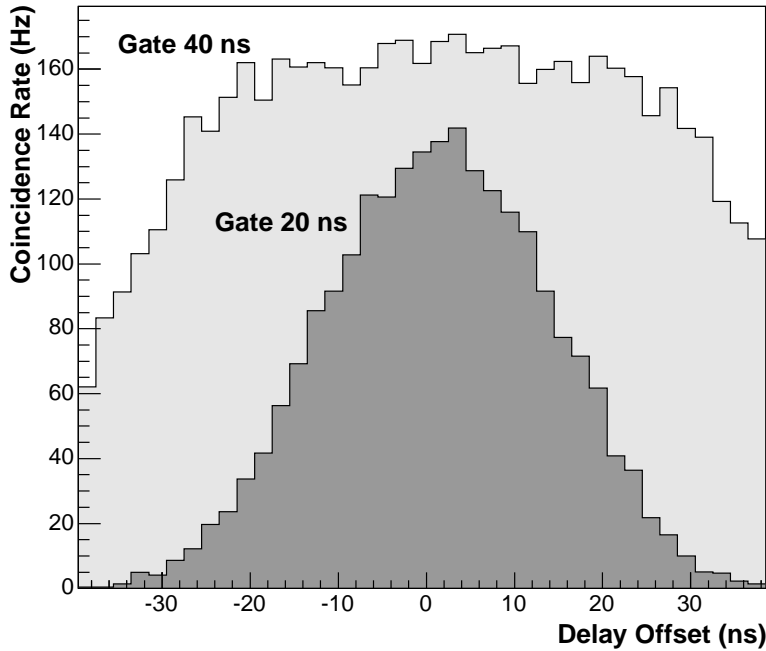


Fig. 4. System rate versus relative delay between a pair of telescopes for coincidence windows of 20 ns and 40 ns.

4.2 *Dead-time Determination*

For the determination of spectra and fluxes of astrophysical γ -ray sources, an accurate measurement of the system dead-time is required. Every Cherenkov event triggering the H.E.S.S. array is recorded by the central trigger system - regardless of the readout status of the cameras. The CTS stores information on which telescopes were able to provide data for a given event, as well as on those that triggered but were busy with the readout of a previous event. This information is used to determine the system dead-time.

Figure 5 shows the distribution of time differences between consecutive events in a run involving only a single telescope. The distribution of all triggers is well described by an exponential as expected. The distribution of events where the telescope was read out is also exponential but with a sharp cut-off at the camera readout dead-time of $446 \mu\text{s}$.

4.3 *Trigger Threshold and Trigger Rates*

The selection of the trigger threshold has direct implications for the energy threshold of the array. A low energy threshold is clearly desirable for astrophysical reasons, however the trigger threshold must be set high enough that

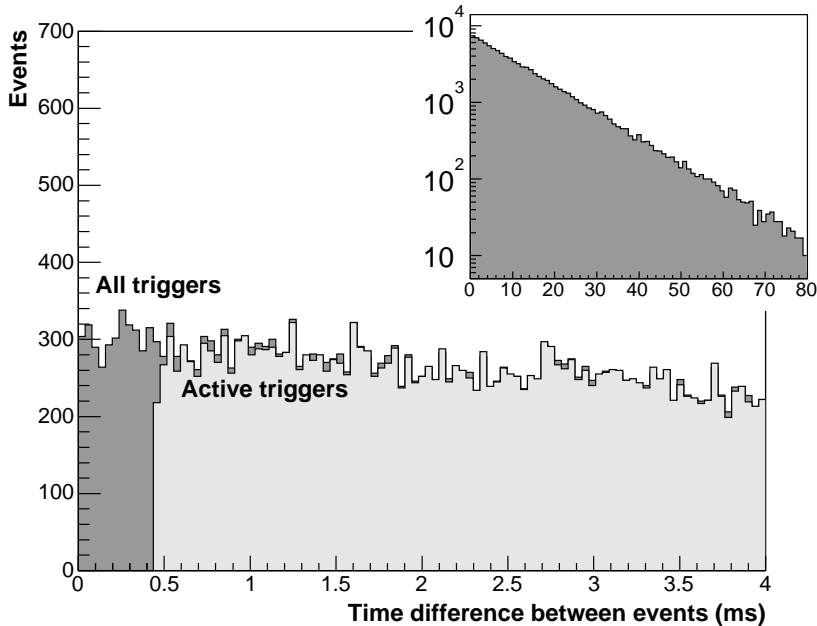


Fig. 5. Distribution of time differences between consecutive events for a single telescope. The dark grey histogram shows all events triggering the system, the light grey histogram shows only events for which the telescope was read out. The inset shows the same distributions but with a logarithmic scale to highlight the exponential behaviour.

the trigger rate is both stable and manageable. In the low threshold regime where night sky background triggers dominate, the rate is expected to be both very high and unstable. Measurements of the dependence of the system trigger rate on all available parameters dictating the threshold are therefore crucial in determining the optimal operating parameters.

The adjustable parameters which directly affect the energy threshold and trigger rate of the system are: the camera pixel and sector thresholds (see section 2.2), and the telescope multiplicity requirement. The measurements described below involve variation of these parameters. All were made with all four telescopes of the system tracking a relatively dark region of the sky close to zenith.

Figure 6 shows how the rates of individual telescopes and the system rate depend on the pixel threshold. Curves are shown for minimum telescope multiplicities of 2 and 3. The pixel threshold is quoted in units of photoelectrons (p.e.), defined as the mean amplitude of a single photoelectron signal at the pixel comparator (21 mV). In all curves, two regimes are clearly present: a smooth power law dependence at higher thresholds and a rapid increase in rate below ≈ 4 p.e. For low pixel thresholds, the camera triggers are dominated by pixel coincidences due to night sky background fluctuations and the system rate is dominated by accidental telescope coincidences. For higher pixel

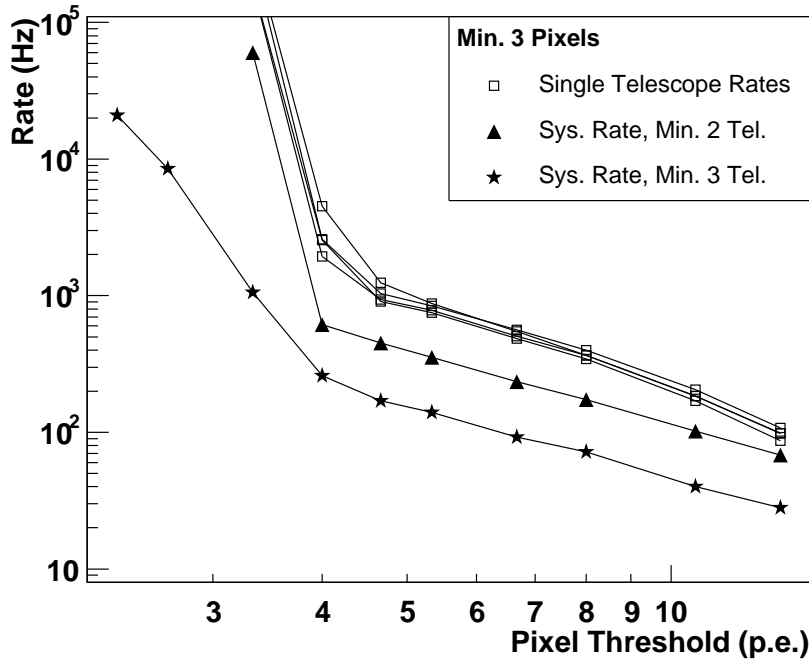


Fig. 6. Single telescope rates and system rate (for a sector threshold of 3 pixels) against pixel threshold. The system rate is shown for telescope multiplicities 2 and 3. Statistical error bars are in all cases smaller than the symbols.

thresholds, random pixel coincidences in the cameras are rare and Cherenkov events from cosmic ray air-showers dominate.

The small dispersion in single telescope rates (in the air-shower dominated regime) that is evident in figure 6 demonstrates the homogeneity of the array. Inter-telescope differences in mirror reflectivity and pixel efficiency are at a level of less than 10%.

Figure 7 shows a comparison of system rate versus pixel threshold for three sector thresholds (pixel multiplicities). For a threshold of 2 pixels, the transition between the NSB and air-shower regimes is rather gradual. For such a condition the system trigger may be affected by NSB fluctuations for a wide range of possible pixel thresholds. As expected, at a higher sector threshold of 4 pixels, a lower operating pixel threshold is attainable. For sector multiplicities of 3 and 4, similar minimum image sizes and system trigger rates are attainable (within the air-shower dominated regime). As a sector threshold of 3 preferentially selects the more compact images typical of gamma-ray initiated showers, this threshold is preferred.

Figure 7 also shows the expected rate of accidental coincidences for a sector threshold of 3 pixels, calculated using the measured single telescope rates and the system coincidence window of 80 ns. The measured system trigger rate at a 3.4 photoelectron threshold is in good agreement with the predicted

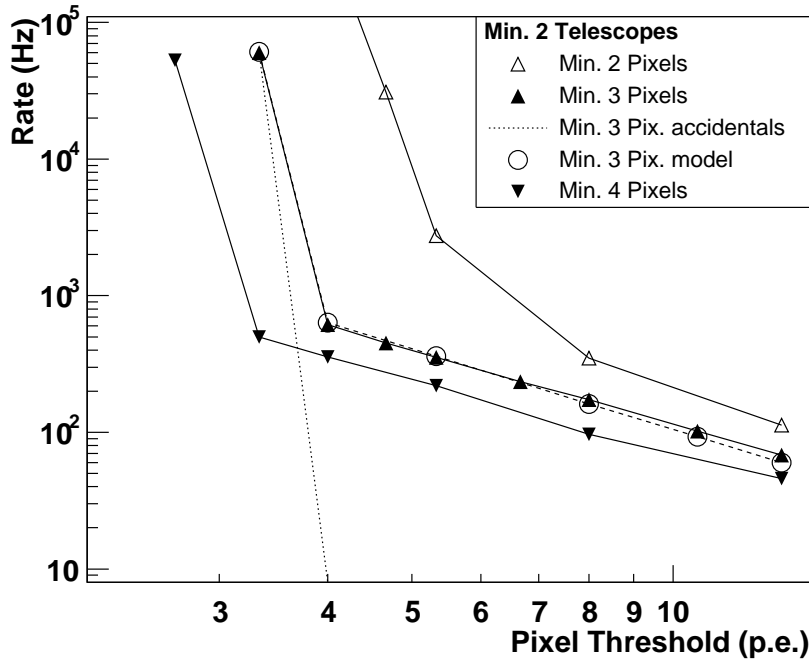


Fig. 7. System trigger rate against pixel threshold for three sector thresholds. For a sector threshold of 3 pixels the predicted rate from accidental telescope coincidences is shown along with the simulated rate for this configuration (open circles). The statistical error bars are smaller than the symbols for all measured curves.

rate of accidentals, indicating that the system trigger behaves as expected, even at this extremely high rate (50 kHz). The open circles show the system trigger rate predicted by Monte Carlo simulations using the CORSIKA [13] air-shower simulation and an optical ray tracing and electronics simulation of the H.E.S.S. telescopes [14] (combined with the expected accidental rate). The comparison of the predicted and measured rates provides an end-to-end test of the simulations and the good agreement is encouraging.

The measurements described above were all made in a relatively dark region of the sky, away from the galactic plane. In such regions the median pixel NSB determined from pixel currents [16] is close to 9.2×10^7 photoelectrons s^{-1} per pixel, compared with the expected value of $8.5 \pm 1.3 \times 10^7$ photoelectrons s^{-1} per pixel [17]. However, as γ -ray observations of all parts of the sky are planned with H.E.S.S., the system must operate stably in much brighter regions of the sky. In a field-of-view with many bright stars or with increased diffuse emission, NSB triggers may occur at higher pixel threshold than in a dark region. To study this effect, the rate versus threshold measurements described above were repeated in the particularly bright region around η Carinae. In this region the transition to NSB dominance occurs close to 4.7 p.e. for a sector threshold of 3 pixels.

To avoid significant NSB trigger rates in bright regions of the sky and as a compromise between higher γ -ray collection efficiency and reduced energy threshold, a configuration of sector threshold 3, pixel threshold 5.3, and telescope multiplicity 2 was chosen for H.E.S.S. observations.

4.4 *Zenith Angle Dependence*

The measurements described in the previous section were performed close to zenith. Standard H.E.S.S. observations take place in a zenith angle range of 0-35°. In certain circumstances this range is extended as far as 60°. At large zenith angles, air-showers are observed through a much greater atmospheric column depth. Cherenkov photons from such showers suffer more from scattering and absorption and have a larger (and dimmer) footprint on the ground. As a consequence of the reduced density of photons in the light pool, the effective energy threshold of the system is increased. On the other hand, the larger light pool diameter results in an improved effective collection area.

Figure 8 shows the rate of the system (and the mean single telescope rate) as a function of the cosine of the zenith angle. A smooth, monotonic decrease is evident for the single telescope and multiplicity-2 rates as expected from the increasing absorption of showers and the steep energy spectrum of the hadronic background. The solid and dashed lines in figure 8 shows the predicted behaviour assuming two different atmospheric transmission tables calculated using MODTRAN [15]. The solid line is based on a rather conservative assumption of aerosol content (maritime haze, boundary layer starting at sea level). The dotted line corresponds to a clearer atmosphere (desert haze, boundary layer starting at 1800 m). The difference between the two predictions indicates the current uncertainty in our understanding of the atmosphere at the H.E.S.S. site.

The increased diameter of the Cherenkov light pool at large zenith angles leads to an increased average telescope multiplicity. This effect is apparent from a comparison of the telescope multiplicity-2 rate with the curves for larger telescope multiplicity in figure 8, indeed the multiplicity-4 rate reaches its maximum at 40° zenith angle.

4.5 *Convergent Telescope Pointing*

The simplest pointing strategy for a telescope array is to track a target with all telescope axes parallel. All measurements described above employed this observation mode. However, given a typical emission height of Cherenkov photons ~ 10 km above the observation level, a more effective strategy may be to

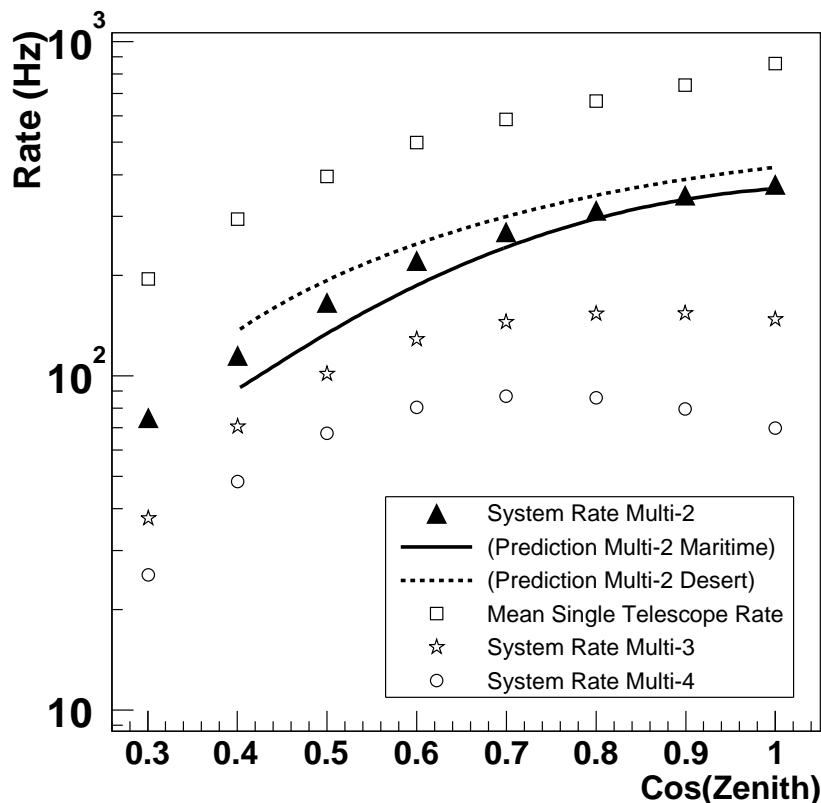


Fig. 8. Mean single telescope and system rate against cosine zenith for telescope multiplicities of 2, 3 and 4. The solid and dashed lines show the rate predicted for multiplicity-2 using two different atmospheric models. These data were taken with telescopes pointing to the north. All statistical error bars are smaller than the plotted symbols.

cant the telescopes towards each other slightly [18]. Given the altitude and array spacing of H.E.S.S., the convergent angle required to maximise the overlap of the telescope field-of-views at the height of maximum shower development is around 0.7° . Figure 9 shows the measured dependence of system trigger rate on the canting angle between telescopes. The maximum trigger rate occurs at a canting angle of 0.65° , corresponding to convergence at a point 10.5 km above the H.E.S.S. site. The solid curve shows a fit of a simple geometrical model of overlapping telescope field-of-views.

Maximising the overlap of telescope field-of-views results in γ -ray images that typically lie closer to the centre of the cameras and increases the average number of usable images in the analysis. This in turn leads to improved angular resolution and hence to better sensitivity. Convergence to a fixed atmospheric depth of 270 g cm^{-2} (the depth of maximum Cherenkov photon emission for an average 100 GeV γ -ray shower) is planned for future H.E.S.S. observations.

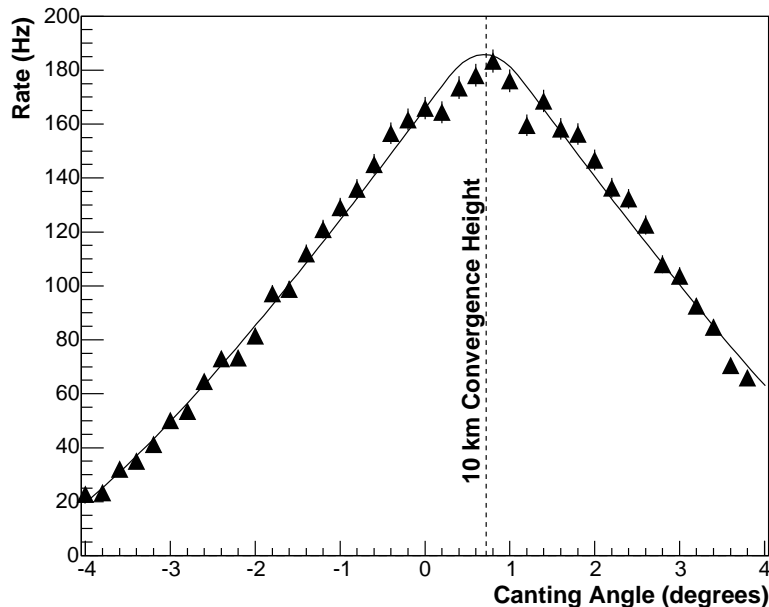


Fig. 9. System rate as a function of the relative alignment of the telescope axes for two telescopes separated by 120 m. The inclination of the telescopes takes place in the plane connecting the two telescopes. Positive values refer to convergent telescope pointing. The solid line is a fit to the data of a simple geometrical model.

5 Implications for System Performance

The operation of a multiplicity-2 telescope trigger for the H.E.S.S. system has many implications. A major consequence is the removal of single muon events at the trigger level. Single muon images have a characteristically narrow distribution of surface brightness. As a consequence they are limited to a small region in the parameter $(\text{image length})/(\text{image size})$ (following the definition of image parameters of Hillas [19]). Figure 10 shows the distribution of $\text{length}/\text{size}$ with and without a telescope multiplicity requirement for fixed camera trigger conditions. For telescope multiplicity-1 there is a large peak at around 3×10^{-5} radians/photoelectron. This peak is produced by images of single muons as can be seen by comparison with the curve for simulated muons shown in figure 10. The tail to the right of the peak is likely produced by more complex shower images that are still dominated by a single muon. From the telescope multiplicity-2 curve in figure 10 it is clear that a multi-telescope trigger is extremely effective at removing such background events; the peak attributed to single muon images is almost completely absent.

The reduction in background evident in figure 10 leads to a lower system trigger rate at a given threshold and hence to reduced readout dead-time. Figure 11 compares the incurred system dead-time versus pixel threshold with and without a telescope multiplicity requirement.

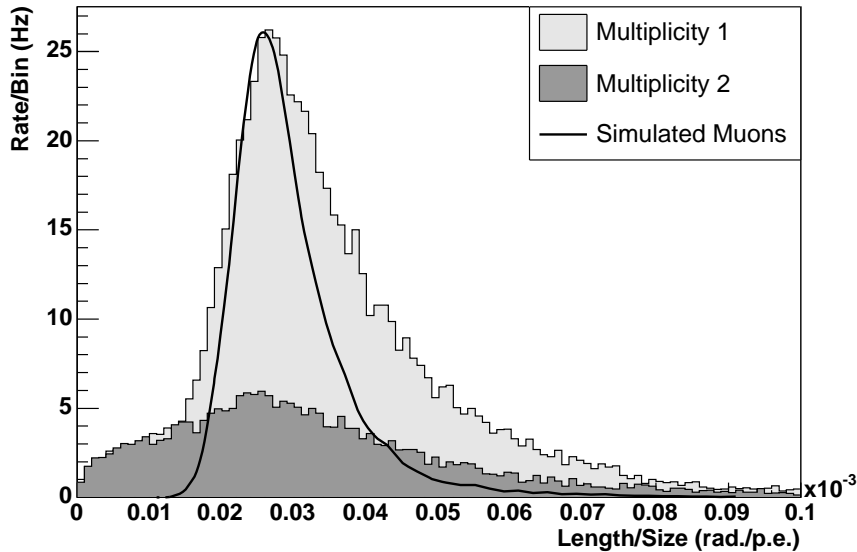


Fig. 10. Distribution of $length/size$ of images for telescope multiplicity 1 and 2. The distribution of simulated single muons is shown by the solid curve.

The dashed line shows the dead-time, calculated defining a *live* system trigger as one where at least 2 telescopes were read out. For the solid curve a more conservative requirement, that all triggered telescopes were read out, was applied. To achieve an acceptable dead-time fraction of 10–15% without a system level trigger, the pixel threshold would have to be increased by a factor ~ 2 . As the energy threshold of the instrument scales roughly with the pixel threshold, operation of H.E.S.S. with a central trigger significantly increases the sensitive energy range of the array.

During the construction and commissioning phase of H.E.S.S., γ -ray observations have been made using several array configurations. The improvements in performance associated with the development of H.E.S.S. from a single telescope system to a full array, are illustrated in table 1. The rate of γ -rays expected from the Crab Nebula is used as a figure of merit in this table. Observations of the Crab Nebula by H.E.S.S. have been used to confirm the performance predicted by air-shower and detector simulations. The improvement in performance between the *2-Tel. Soft.* and *2-Tel. Hard.* configurations is solely a consequence of the introduction of the system level trigger.

Figure 12 illustrates the decreasing energy threshold of the array during the commissioning phase. With the complete 4-telescope H.E.S.S. phase-I system a hardware energy threshold of 100 GeV is achieved at zenith. After γ -ray selection cuts the threshold increases to 125 GeV. In comparison, the post-cuts threshold for data taken with a single H.E.S.S. telescope is 265 GeV. For this configuration a $length/size$ cut is imposed to reject single muons off-line, at the expense of an increased analysis threshold.

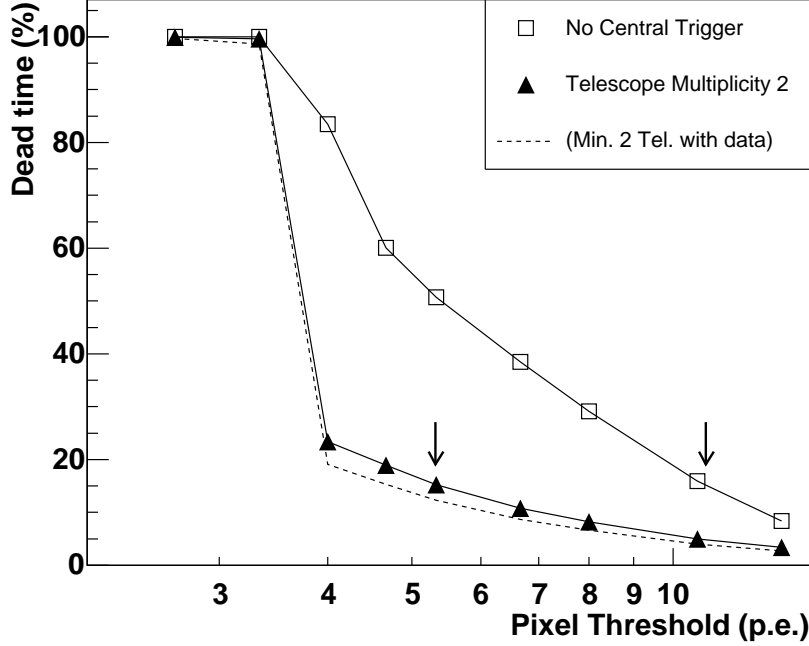


Fig. 11. Derived system dead-time as a function of pixel trigger threshold (for a fixed sector threshold of 3 pixels), with and without a system level trigger. The dashed and solid curves are calculated using different definitions of the system dead-time (see text). The left arrow shows the current operating pixel threshold of H.E.S.S., the right arrow shows the threshold corresponding to the same system dead-time with no telescope multiplicity requirement.

6 Summary

The system level trigger of the H.E.S.S. detector provides an effective suppression of background events at the hardware level and pre-selects events for stereoscopic reconstruction. This background rejection enables the operation of H.E.S.S. with a lower dead-time and at a lower energy threshold for the detection of γ -rays. The combination of large mirror area, fast camera electronics, and stereoscopy has allowed the first phase of the H.E.S.S. project to achieve its target energy threshold of 100 GeV.

Acknowledgements

The authors would like to acknowledge the support of their host institutions, and additionally support from the German Ministry for Education and Research (BMBF), the French Ministry for Research, and the Astroparticle Interdisciplinary Programme of the CNRS. We appreciate the excellent work of

Configuration	Camera Trigger Condition	System Rate (Hz)	Crab γ -ray Rate (min^{-1})		
			Predicted		Measured
			Pre-cuts	Post-cuts	Post-cuts
Single Telescope	6.7 pe, 4 pix	170	9.1 ± 1.6	3.0 ± 0.5	3.8 ± 0.1
2-Tel. Soft.	6.7 pe, 4 pix	50 (280)	5.6 ± 1.0	3.6 ± 0.7	
2-Tel. Hard.	5.3 pe, 3 pix	90	13.5 ± 2.4	6.7 ± 1.2	
3-Tel. Hard.	5.3 pe, 3 pix	180	20.2 ± 3.7	11.8 ± 2.1	10.4 ± 0.3
4-Tel. Hard.	5.3 pe, 3 pix	270	25.9 ± 4.7	15.6 ± 2.8	

Table 1

Comparisons of the performance of different H.E.S.S. configurations. The typical system trigger rate is given together with the predicted (and measured) γ -ray rate from the Crab Nebula (at 47° zenith angle). The predicted rates are calculated using the spectrum published by the HEGRA collaboration [20], the errors shown are statistical only. *Soft.* and *Hard.* refer to software and hardware 2-telescope multiplicity requirements. For the *2-Tel. Soft.* configuration the trigger rate including single telescope events is shown in parentheses.

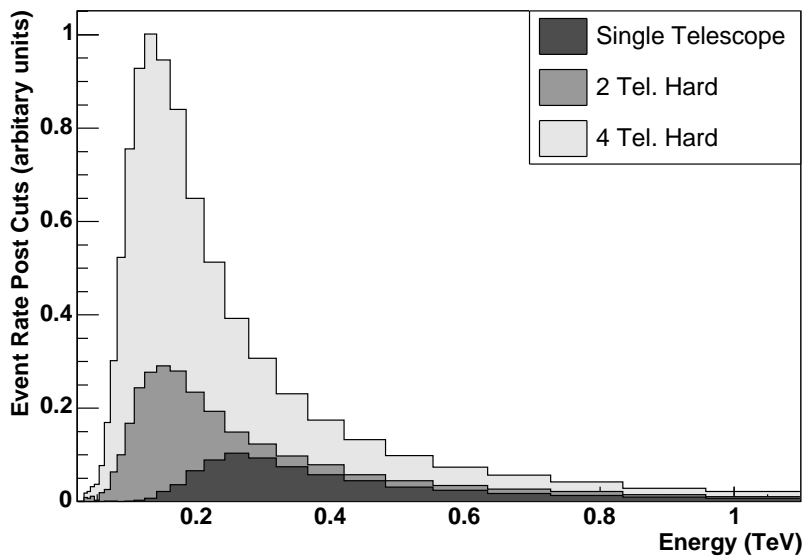


Fig. 12. Post-cuts differential rate expected on the basis of detailed simulations for a Crab-like source at zenith, for different H.E.S.S. configurations. The energy threshold is conventionally defined as the peak in this distribution and is 265 GeV, 145 GeV and 125 GeV for the single telescope, 2-telescope and 4-telescope configurations respectively.

the electronic engineering and technical support staff in Heidelberg (in particular, T. Schwab and N. Bulian), in Paris, and in Namibia in the construction and operation of the equipment. We acknowledge the support of S. Schlenker during the measurement campaign.

References

- [1] Weekes, T.C. *et al.*, 1989, *Astrophys. J.* **342**, 379.
- [2] Daum, A. *et al.*, 1997, *Astropart. Phys.* **8**, 1.
- [3] Hinton, J.A. (*H.E.S.S. Collaboration*), 2004, *New Astron. Rev.* **48**, 331.
- [4] Weekes, T.C. *et al.*, 2002, *Astropart. Phys.* **17**, 221.
- [5] Kubo, H. *et al.*, 2004, *New Astron. Rev.* **48**, 323.
- [6] Lorenz, E. (*MAGIC Collaboration*), 2004, *New Astron. Rev.* **48**, 339.
- [7] Bernlöhner, K. *et al.*, 2003, *Astropart. Phys.* **20**, 111.
- [8] Vincent, P. *et al.*, 2003, *Proc. 28th ICRC (Tsukuba)*, Univ. Academy Press, Tokyo. p. 2887.
- [9] Aharonian, F.A. *et al.*, 1999, *Astron. & Astrophys.* **349**, 11.
- [10] Bulian, N. *et al.*, 1998, *Astropart. Phys.* **8**, 223.
- [11] Feinstein, F. (*ANTARES Collaboration*), *Nucl. Instrum. Meth. A* **504**, 258.
- [12] Franzen, A. *et al.*, 2003, *Proc. 28th ICRC (Tsukuba)*, Univ. Academy Press, Tokyo. p. 2987.
- [13] Heck, D. *et al.*, 1998, *Forschungszentrum Karlsruhe Report* **FZKA 6019**.
- [14] Bernlöhner, K. 2004, In preparation.
- [15] Bernlöhner, K. 2000, *Astropart. Phys.* **12**, 255.
- [16] Aharonian, F.A. *et al.*, 2004, Submitted to *Astropart. Phys.*
- [17] Preuss, S. *et al.*, 2002, *Nucl. Instrum. Meth. A* **481**, 229.
- [18] Lampeitl, H. *et al.*, 1999, *AIP Proc. GeV-TeV Gamma Ray Astrophysics Workshop (Snowbird)*, **515**, 328 (astro-ph/9910461).
- [19] Hillas, A. M. 1985, *Proc. 19th ICRC (La Jolla)* **3**, 445.
- [20] Aharonian, F.A. *et al.*, 2000, *Astrophys. J.* **539**, 317.